ISBN: 978-3-95450-229-5 ISSN: 2673-5520 doi:10.18429/JACoW-MEDSI2020-MOPC13

RECENT STUDIES ON THE VIBRATION RESPONSE OF NSLS-II GIRDER SUPPORT SYSTEM

S. Sharma† and C. Spataro, NSLS-II, Brookhaven National Laboratory, Upton, NY, USA

Abstract

The designs of various girder support systems were reviewed recently in a MEDSI School tutorial [1]. A comparison of their horizontal transmissibility values in (2-100 Hz) band showed that the NSLS-II girder support system had a lower transmissibility despite its first natural frequency being the lowest (~30 Hz). Detailed vibration tests and finite element (FE) analyses have been performed to understand this anomaly and to assess the role of viscoelastic damping pads underneath the NSLS-II girders. The analyses were extended to include harmonic response analysis to model viscoelastic properties, and to random vibration analysis to obtain uncorrelated motions between the magnets. The results of these new tests and FE analyses are discussed in this paper.

INTRODUCTION

Ambient floor motion is one of the major sources of beam stability perturbations in the storage rings. The floor motion is magnified by high transmissibility ratios of the girder-magnet assemblies at their natural frequencies. At higher frequencies, the floor motion reduces exponentially [2] as $1/f^n$ with exponent n = 4. Therefore, the girder support systems are usually designed with the requirement of high natural frequencies, specifically the 1st natural frequency of > 30 Hz. Girder support systems with higher 1st natural frequencies (see Table 1) are expected to have lower broadband (2 – 100 Hz) transmissibility ratios.

Table 1: Comparison of 1st Natural Frequencies and Transmissibility Ratios in (2 – 100 Hz) Band

Facility	1st Nat. Freq.	Trans. (H)	Trans. (V)
NSLS-II	30 Hz	1.03*	1.01
APSU !	42 Hz	1.30	1.01
ESRF	42 Hz	1.24	1.21
TPS	44 Hz	1.20	1.01
SIRIUS	133 Hz	1.39	1.07

*Corrected to 1.07 !Estimated from FE Model

A low transmissivity ratio of 1.03 for NSLS-II girders in the horizontal direction appeared to be inconsistent with a lower 1st natural frequency, $f_{n,1}$, of 30 Hz. Additional vibrations tests were performed at NSLS-II in December 2019 and March 2020. The transmissibility ratio was corrected to 1.07 to account for a calibration difference between the seismometers in the very low frequency range of (2 – 4 Hz), but the apparent discrepancy was still significant.

The design of NSLS-II girder support system is unique in its use of viscoelastic pads for thermal stability. For any fluctuation in the tunnel-air temperature, or the floor temperature, the viscoelastic pads allow the girders to expand or contract without bending, thereby minimizing magnet-to-magnet misalignment [3, 4]. Although not intended for vibration damping, they are expected to have some effect on reducing the transmissibility ratios. This was investigated by vibration tests and FE models as described in the following sections.

NSLS-II GIRDER-MAGNET ASSEMBLY

A typical NSLS-II multipole girder-magnet assembly is shown in Fig. 1(top). The girder is supported on 2-inch diameter threaded rods at 4 locations approximately 1.2 m apart. Multiple support points increase the stiffness of the girder and raise its natural frequencies. At the bottom, the threaded rods are bolted to a solid 2.5-inch steel plate at the 2nd location from the upstream end, and to viscoelastic pads (Fig. 1(bottom)) at the other locations.

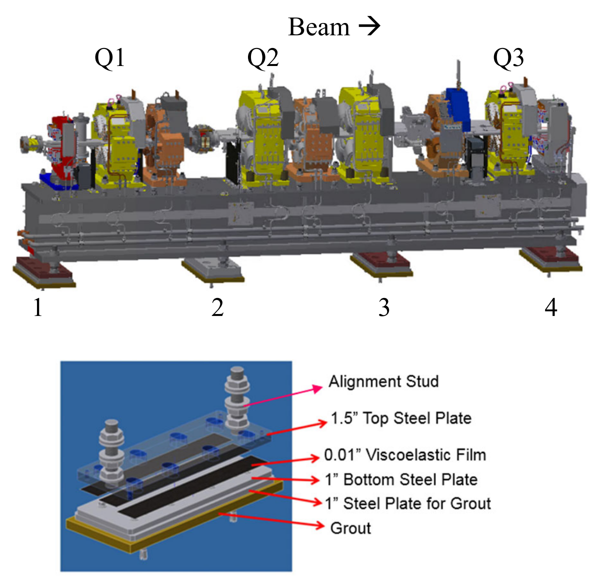

Figure 1: A typical NSLS-II girder (top) is supported at 4 locations. Viscoelastic pads (bottom) are used at locations 1, 3 and 4.

Viscoelastic pads consist of two steel plates, 1.5-inch thick (top) and 1.0-inch thick (bottom), joined by 0.01-inch thick viscoelastic films, brand-name VHB F9469PC, made by 3M®. Experimental data for the storage and loss moduli [5] for this film are plotted in Fig. 2.

FE MODELING OF VISCOELASTIC FILM

In Ansys FE models, viscoelastic properties can be expressed as shear and bulk relaxation moduli (*G(t)* and *K(t)*) in Prony series:

$$G(t) = G_\infty + \sum_{i=1}^{n} G_i \, exp\left(-\frac{t}{\tau_i^G}\right) \quad (1)$$

$$K(t) = K_\infty + \sum_{i=1}^{n} K_i \, exp\left(-\frac{t}{\tau_i^K}\right) \quad (2)$$

† sharma@bnl.gov

Content from this work may be used under the terms of the CC BY 3.0 licence (© 2021). Any distribution of this work must maintain attribution to the author(s), title of the work, publisher, and DOI

ISBN: 978-3-95450-229-5 ISSN: 2673-5520 doi:10.18429/JACoW-MEDSI2020-MOPC13

Content from this work may be used under the terms of the CC BY 3.0 licence (© 2021). Any distribution of this work must maintain attribution to the author(s), title of the work, publisher, and DOI

where coefficients of the Prony series ($G(\infty), K(\infty), Gi, Ki, \tau_i^G, \tau_i^K$) are determined from experimental storage and loss moduli provided as input data.

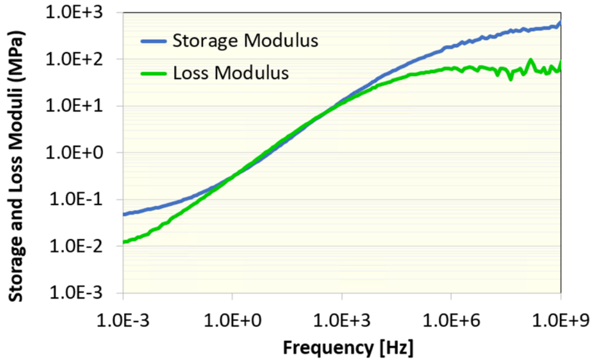

Figure 2: Storage and loss moduli of VHB F9469PC® viscoelastic film versus frequency [5].

Viscoelastic material models can be used in Ansys harmonic response analysis but not in random vibration analysis. Therefore, in random vibration analysis the effect of viscoelastic damping was included indirectly. The girder-magnet assembly was first modelled without the viscoelastic films with structural damping ratio decreasing with frequency. Based on past experimental data, the damping ratio was approximated as 0.01 (1 - 40 Hz), 0.005 (40 - 80 Hz) and 0.0025 (80 – 110 Hz). Harmonic response analyses with horizontal base excitation were then performed including viscoelastic films in the FE model. Finally, the damping contribution of the viscoelastic films was simulated by increasing the frequency dependent damping ratios while using only the elastic properties of the films. The resulting equivalent damping ratios were established as: 0.035 (1 - 40 Hz), 0.02 (40 - 80 Hz) and 0.0075 (80 - 110 Hz), representing a factor of ~ 3 increase over the initial damping ratios. Harmonic responses for the Q3 magnet (Fig. 1) for the three different cases of damping are compared in Fig. 3. Peak transmissibility values at the natural frequencies show that equivalent damping ratios can represent the viscoelastic damping effect reasonably well.

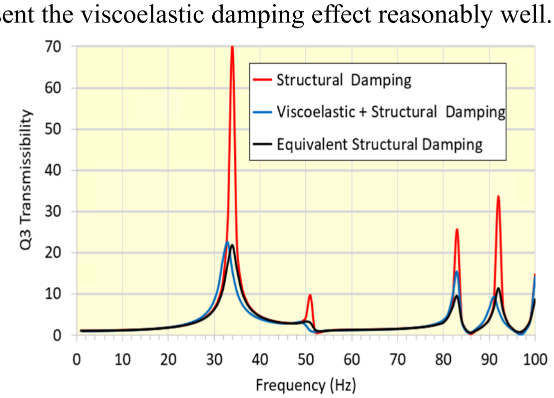

Figure 3: Horizontal transmissibility ratio of Q3 magnet for 3 different cases of damping, (1) structural, (2) structural + viscoelastic, and (3) equivalent structural.

RANDOM VIBRATION ANALYSIS

Natural frequencies of the girder-magnet assembly were first calculated as a prerequisite for the random vibration analysis. The first five natural frequencies, $f_{n,1}$ to $f_{n,5}$, with their mode shapes are shown in Table 2. Higher modes (f_n > 100 Hz) are not included since the floor motion above 100 Hz is negligible.

Table 2: Natural Frequencies and Mode Shapes

$f_{n,i}$	FE Analysis (Hz)	Experimental (Hz)	Mode Shape (X, Y, Z: Hor., Ver., Beam)
1	30.4	30.0	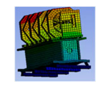 X-Translation – Roll
2	46.4	43.8	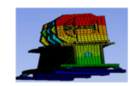 Yaw
3	66.6	61.9	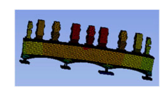 Bend (Y-Z Plane)
4	81.3	77.5	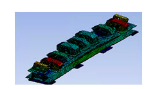 Bend (X-Z Plane)
5	84.1	89.1	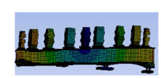 Pitch

The calculated natural frequencies and equivalent damping ratios were used in the random vibration FE model. Input motion at the base was applied as two separate PSDs at the support locations (1,2) and (3,4) because at NSLS-II the floor motion is not correlated above 10 Hz for a distance of > 2 m [6]. Experimental floor PSDs were obtained with Sercel (model L4-C) seismometers.

Measured and calculated PSDs in the horizontal direction for the Q3 magnet are plotted in Fig. 4 together with the floor PSD.

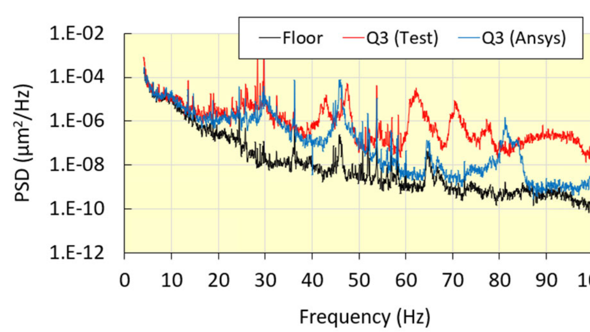

Figure 4: Measured (red) and calculated (blue) PSDs of Q3 magnet in the horizontal direction. PSD of the floor used as input in the FE analysis is also shown (black).

Figure 4 shows a good agreement between the experimental and FE analysis data for frequencies below 50 Hz. The agreement is poor above 60 Hz with more peaks in the test data. The floor motion above 50 Hz is small, 0.5 nm

ISBN: 978-3-95450-229-5 ISSN: 2673-5520 doi:10.18429/JACoW-MEDSI2020-MOPC13

rms compared to 13.3 nm rms in (4-50 Hz) band, and its effect on the integrated motion and transmissibility ratio is also comparatively small. The peaks at the first two natural frequencies, (30.4 Hz and 46.4 Hz) are damped substantially by the high equivalent damping ratios provided by the viscoelastic pads. This results in overall low transmissibility ratios of the NSLS-II girder-magnet assemblies (Table 1).

UNCORRELATED MOTION

At NSLS-II the vibration specification is given as uncorrelated motion between the end quadrupoles on the girder, Q1 and Q3, (Fig. 1). In the horizontal direction the rms value in (2–100 Hz) band is specified to be < 150 nm. For the upgrade of NSLS-II this value is expected to be an order of magnitude lower.

Uncorrelated rms motion between the quadrupoles can be readily measured on prototypes or in-service girder-magnet assemblies. However, in a random vibration FE analysis, the rms motions for the magnets contain no phase information. Uncorrelated motion between the magnets is, therefore, not available to evaluate different girder designs with respect to this specification. The following approach is being evaluated to address this for the future upgrade of NSLS-II.

Correlation coefficient between Q1 and Q3 is plotted in Fig. 5 from a recent (December 2019) set of test data. The correlation coefficient is ~ 1.0 up to the first natural frequency of 30 Hz. The girder can be assumed to be rigid in (2 - 30 Hz) band with no relative motion between Q1 and Q3. Above 30 Hz, the correlation coefficient drops sharply with its value fluctuating between roughly equal positive and negative values. Conservatively it can be assumed that the uncorrelated rms motion between the two magnets is the SRSS of their integrated rms motions in (30 – 100 Hz) band.

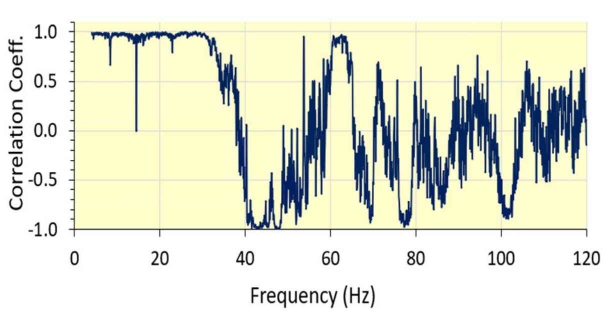

Figure 5: Correlation coefficient between Q1 and Q3 magnets.

FE analysis results for the integrated rms motions of Q1 and Q3 in the (30-100 Hz) band are plotted in Fig. 6. A large fraction of the motion occurs at 46.4 Hz in the yaw mode in which Q1 and Q3 move in the opposite directions. With integrated motions of 15.5 nm for Q1 and 7.5 nm for Q3, an uncorrelated motion of 17.2 nm is obtained. In comparison, the measured value of uncorrelated motion in the (4 - 100 Hz) band was 18.2 nm.

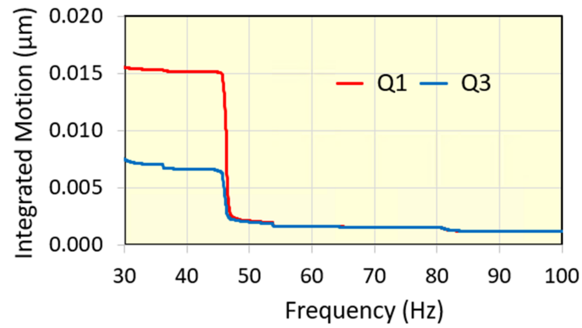

Figure 6: FE analysis results for the integrated rms motions of Q1 and Q3 in (30 - 100 Hz) band. A large fraction of the motion occurs in the yaw mode at 46.4 Hz.

CONCLUSION

FE analyses and experiments were performed to investigate the low transmissibility ratio of the NSLS-II girder support system. Viscoelastic films in the support pads were modelled using experimental storage and loss moduli. The results show that viscoelastic pads increase the effective damping ratio of the girder by a factor of ~ 3, thus lowering its transmissibility ratio. Relative motion between the quadrupole magnets was essentially uncorrelated above the 1st natural frequency (~ 30 Hz). From random vibration analysis the uncorrelated quadrupole motion was estimated as 17.2 nm.

ACKNOWLEDGEMENTS

This work has been supported by the U.S. Department of Energy, Office of Science, under contract number DE-SC0012704.

The authors thank Q. Yuan and A. Cotter of 3M® Corporations for providing technical data and guidance on VHB viscoelastic films. Many discussions with James Dymoke-Bradshaw of the Diamond Light Source were helpful in performing vibrations tests and interpreting the results.

REFERENCES

[1] S. Sharma, “Storage ring issues for low-emittance storage rings,” presented at *MEDSI School 2*, Grenoble, France, 2019. https://medsi.lbl.gov/SysIncludes/retrieve.php?url=https://medsi.lbl.gov/files/page_164/Sharma_SupportSystem_Alignment_Stability_Oct18_2019.pdf

[2] A. Seryi, “Ground motion and vibration issues for accelerators,” in *Proc. PAC2001*, Chicago, IL, USA, June 2001, paper WOAB009, pp. 364-368.

[3] V. Ravindranath *et al.*, “Stability of NSLS-II girder-magnet assembly,” in *Proc. MEDSI2010*, Oxford, England, UK, October 2011. http://dx.doi.org/10.1017/S2044820110000675

[4] S. Sharma *et al.*, “Optimization of magnet stability and alignment for NSLS-II,” in *Proc. PAC2011*, New York, NY, USA, March-Apr 2011, paper THOBS2, pp. 2082-2086.

[5] Q. Yuan and A. Cotter, 3M® Corporation, Private Communication, March 2020.

[6] C. Spataro *et al.*, “Recent site vibration studies at NSLS-II,” presented at *MEDSI2014* , Melbourne, Australia, October

Content from this work may be used under the terms of the CC BY 3.0 licence (© 2021). Any distribution of this work must maintain attribution to the author(s), title of the work, publisher, and DOI

ISBN: 978-3-95450-229-5 ISSN: 2673-5520 doi:10.18429/JACoW-MEDSI2020-MOPC13

Content from this work may be used under the terms of the CC BY 3.0 licence (© 2021). Any distribution of this work must maintain attribution to the author(s), title of the work, publisher, and DOI

2014. https://medsi.lbl.gov/SysIncludes/retrieve.php?url=https://medsi.lbl.gov/files/page_156/Presentations/Recent_Site_Vibration_Studies_at_NSLS_II_Sushil_Sharma